

Hyun Woo Goo  
Choong-Gon Choi

## Post-contrast FLAIR MR imaging of the brain in children: normal and abnormal intracranial enhancement

Received: 15 June 2003  
Revised: 22 July 2003  
Accepted: 26 July 2003  
Published online: 10 October 2003  
© Springer-Verlag 2003

Presented at the 46th Annual Meeting of the Society for Pediatric Radiology, San Francisco, California, USA, May 2003

H.W. Goo (✉) · C.-G. Choi  
Department of Radiology,  
Asan Medical Center,  
University of Ulsan College of Medicine,  
388-1 Poongnap-dong, Songpa-gu,  
Seoul, Korea  
E-mail: hwgoo@amc.seoul.kr  
Tel.: +82-2-2224-4388  
Fax: +82-2-476-4719

**Abstract Objective:** To describe the normally enhancing intracranial structures on fluid-attenuated inversion recovery (FLAIR) MRI and evaluate the usefulness of postcontrast FLAIR images of the brain in the assessment of enhancing lesions by comparing postcontrast FLAIR imaging with postcontrast T1-weighted (T1-W) imaging in children. **Materials and methods:** In 218 children, 249 pre- and postcontrast FLAIR MRI examinations of the brain were obtained consecutively between August 2001 and April 2002. The normally enhancing intracranial structures on FLAIR imaging were assessed in 77 MRI studies of 74 children who showed normal intracranial imaging findings. In 86 MRI studies in 68 children who showed enhancing intracranial lesions, lesion conspicuity on postcontrast FLAIR imaging was compared with that on postcontrast T1-W imaging for all lesions ( $n=107$ ), intra-axial lesions ( $n=40$ ), or extra-axial lesions ( $n=67$ ). **Results:** The normally enhancing intracranial structures on FLAIR MRI were the choroid plexus (99%, 76/77), pituitary stalk

(84%, 65/77), pineal gland (71%, 55/77), dural sinuses (26%, 20/77), and cortical veins (9%, 7/77). Of all the enhancing lesions, lesion conspicuousness on postcontrast FLAIR imaging was better than postcontrast T1-weighted imaging in 42, equal in 28, and worse in 37. Of 40 intra-axial lesions, lesion conspicuousness on postcontrast FLAIR imaging was better in 6, equal in 10, and worse in 24. Of 67 extra-axial lesions, lesion conspicuity on postcontrast FLAIR imaging was better in 36, equal in 18, and worse in 13. Conspicuousness of extra-axial lesions was significantly better than that of intra-axial lesions on postcontrast FLAIR imaging ( $P<0.001$ ). **Conclusions:** The choroid plexus, pituitary stalk, pineal gland, dural sinuses, and cortical veins show normal enhancement on postcontrast FLAIR MRI in children, and postcontrast FLAIR imaging appears better than postcontrast T1-W imaging in the assessment of extra-axial enhancing lesions in children.

**Keywords** Brain · Technique · MRI · Children

### Introduction

Postcontrast T1-weighted (T1-W) brain MR imaging is helpful in the detection and characterisation of various

intracranial abnormalities. An enhancing portion in an intra-axial lesion results from a breakdown of the blood-brain barrier and the subsequent leakage of injected paramagnetic contrast agent into the cerebral

extra-vascular space. Contrast enhancement is also seen on fluid-attenuated inversion recovery (FLAIR) brain MR imaging after IV administration of contrast agent. Contrast enhancement on FLAIR imaging is the result of a mild T1 effect, which is produced by the long inversion time used to nullify the signal intensity of water. Moreover, FLAIR imaging has recently been described to be more sensitive than T1-W imaging to low concentrations of gadopentetate dimeglumine [1, 2, 3]. Postcontrast FLAIR imaging has been investigated in the assessment of intra-axial [1, 4, 5, 6, 7] and extra-axial lesions [1, 2, 8, 9, 10, 11, 12, 13, 14, 15]. However, most previous studies included only a small number of paediatric cases. The purpose of this study was to describe the normally enhancing intracranial structures on FLAIR imaging and evaluate the usefulness of postcontrast FLAIR MRI of the brain in the assessment of enhancing lesions by comparing postcontrast FLAIR imaging with postcontrast T1-W imaging in children.

## Materials and methods

In 218 children, 249 pre- and postcontrast FLAIR brain MRI examinations were performed consecutively between August 2001 and April 2002. This study was approved by the institutional review board, and informed consent was not required. MR imaging was performed on a clinical 1.5-T MR system (Magnetom Vision; Siemens Medical Systems, Iselin, N.J. or Signa CV/i; GE Medical Systems, Milwaukee, Wis.). Imaging parameters for fast FLAIR imaging included repetition time of 10,000 ms, effective echo time of 100–130 ms, inversion time of 2,200–2,400 ms, various echo train lengths (7 in 50 studies and 15–20 in 36 studies), section thickness of 5 mm, matrix of 256×192, and one signal acquisition. FLAIR imaging and T1-W imaging was performed 4 min after IV administration of 0.1 mmol/kg of gadopentetate dimeglumine (Magnevist, Schering, Berlin, Germany) in random order. Imaging parameters for T1-W imaging included a repetition time of 400–780 ms and echo time of 8–14 ms, section thickness of 5 mm, matrix of 256×192, and one or two signal acquisitions. Postcontrast T1-W imaging was obtained with standard technique, fat suppression, or magnetization transfer.

The normally enhancing intracranial structures on FLAIR imaging were assessed in 77 MR studies of 74 children (age range 5 days–17 years, mean 6 years; 37 boys, 37 girls), which showed normal intracranial imaging findings on all imaging sequences. The normal intracranial enhancement was visually assessed with a side-by-side comparison of corresponding pre- and postcontrast FLAIR imaging.

In 86 MR studies of 68 children (age range 7 days–17 years, mean 5 years; 30 boys, 38 girls), which showed enhancing intracranial lesions, lesion conspicuousness on postcontrast FLAIR imaging was compared with that on postcontrast T1-W imaging for all lesions ( $n=107$ ), intra-axial lesions ( $n=40$ ), or extra-axial lesions ( $n=67$ ). The diagnosis of enhancing lesion was based on pathological, clinical, or imaging findings. Intra-axial lesions included brain tumour ( $n=18$ ; medulloblastoma [ $n=3$ ], ependymoma [ $n=3$ ], choroid plexus carcinoma [ $n=3$ ], glioma [ $n=2$ ], lymphoma [ $n=2$ ], haemophagocytic lymphohistiocytosis [ $n=2$ ], germ cell tumour [ $n=1$ ], atypical teratoid/rhabdoid tumour [ $n=1$ ], chloroma [ $n=1$ ]), postoperative enhancement ( $n=7$ ), inflammatory lesions ( $n=5$ ; acute disseminated encephalomyelitis

[ $n=4$ ], adrenoleucodystrophy [ $n=1$ ]), infection ( $n=4$ ), infarction ( $n=3$ ), and vascular lesions ( $n=3$ ; venous angiomas [ $n=2$ ], and arteriovenous malformation [ $n=1$ ]).

Extra-axial lesions included postoperative enhancement ( $n=22$ ), meningitis ( $n=14$ ; bacterial meningitis [ $n=12$ ], tuberculous meningitis [ $n=2$ ]), subdural haematoma ( $n=12$ ), leptomeningeal metastasis ( $n=11$ ), vascular lesions ( $n=7$ ; leptomeningeal angiomatosis [ $n=4$ ], moyamoya disease [ $n=2$ ], infarction [ $n=1$ ]), and epidural haematoma ( $n=1$ ). Postcontrast FLAIR imaging was performed before postcontrast T1-W imaging in 62 studies and after postcontrast T1-W imaging in 24 studies. Postcontrast T1-W imaging was obtained with the standard technique in five studies, fat suppression in 50 studies, and magnetization transfer in 31 studies. Two radiologists compared lesion conspicuousness between two sequences and graded postcontrast FLAIR imaging into three ordinal scales (better, equal, or worse) by consensus. The grades of lesion conspicuousness on postcontrast FLAIR imaging were compared between intra-axial and extra-axial lesions using Wilcoxon's rank sum test. A  $P$  value of less than 0.05 was considered to indicate a statistically significant difference.

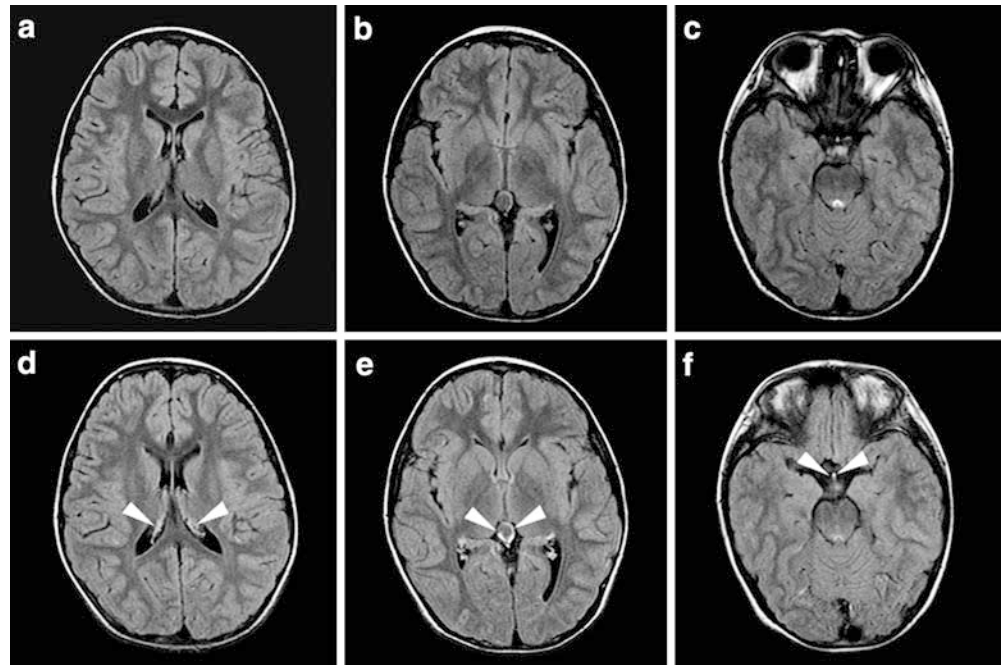
## Results

The normally enhancing intracranial structures on FLAIR MRI were choroid plexus (99%, 76/77), pituitary stalk (84%, 65/77), pineal gland (71%, 55/77), dural sinuses (26%, 20/77), and cortical veins (9%, 7/77) (Fig. 1). However, most of the normal vascular enhancement seen on T1-W imaging was not visible on postcontrast FLAIR imaging. Of all the enhancing lesions, lesion conspicuity on postcontrast FLAIR imaging was better than postcontrast T1-W imaging in 42, equal in 28, and worse in 37. Of 40 intra-axial lesions, lesion conspicuousness on postcontrast FLAIR imaging was better in 6, equal in 10, and worse in 24. Of 67 extra-axial lesions, lesion conspicuousness on postcontrast FLAIR imaging was better in 36, equal in 18, and worse in 13. Conspicuousness of extra-axial lesions was significantly better than those of intra-axial lesion on postcontrast FLAIR imaging ( $P < 0.001$ ).

Among intra-axial lesions, conspicuousness of enhancing lesions on postcontrast FLAIR MRI was worse than that on postcontrast T1-weighted MRI in 72% (13/18) of tumours (Fig. 2), 80% (4/5) of inflammatory lesions, and 100% (3/3) of vascular lesions (Fig. 3) (Table 1). For other intra-axial lesions, including postoperative enhancement, infection and infarction, conspicuousness of enhancing lesions on postcontrast FLAIR imaging was comparable to that on postcontrast T1-W imaging.

Among extra-axial lesions, conspicuousness of enhancing lesions on postcontrast FLAIR imaging was better than that on postcontrast T1-W imaging in 64% (14/22) of postoperative enhancement (Fig. 4), 64% (9/14) of meningitis (Fig. 5), 58% (7/12) of subdural haematomas (Fig. 6), and 75% (3/4) of leptomeningeal angiomatosis (Table 2). Conspicuousness of enhancing lesions on postcontrast FLAIR imaging was comparable

**Fig. 1a–f** A 7-year-old girl with normal intracranial imaging findings. **a–c** Precontrast axial FLAIR MR images at three levels for comparison. **d–f** Post-contrast axial FLAIR images at corresponding levels show normal enhancement in the choroid plexus (**d**, arrowheads), pineal gland (**e**, arrowheads), and pituitary stalk (**f**, arrowheads). Other normal vascular enhancement except for the choroid plexus is not seen. **b,e** A benign non-neoplastic pineal cyst is present



to that on postcontrast T1-W imaging in leptomeningeal metastasis and worse in 100% (3/3) of vascular lesions except for leptomeningeal angiomatosis.

## Discussion

FLAIR MRI provides different signal intensity characteristics for various intracranial abnormalities when compared with conventional MRI [16, 17, 18, 19, 20, 21]. This feature of FLAIR imaging is mainly attributed to the long inversion time attenuating the signal intensity

of fluid and the sequence itself having heavy T2-weighting. Therefore, FLAIR imaging is advantageous in the assessment of intracranial lesions in, or adjacent to, CSF. FLAIR imaging is so sensitive that high inspired oxygen fraction during anaesthesia makes the signal intensity of CSF hyperintense [22]. Recently, postcontrast FLAIR imaging has been investigated in the evaluation of intracranial enhancing lesions [1, 2, 4, 5, 6, 7, 8, 9, 10, 11, 12, 13, 14, 15]. However, to our knowledge, normally enhancing intracranial structures on FLAIR imaging have not been described and intracranial enhancing lesions on FLAIR imaging have also not been evaluated in a large group of children.

**Fig. 2a–c** A 3-year-old girl with medulloblastoma. **a** A precontrast axial FLAIR MR image shows a solid mass in the cerebellar vermis (arrows). The mass is nearly isointense to grey matter. **b** Postcontrast axial FLAIR MR image reveals mild heterogeneous enhancement in the mass. **c** Postcontrast axial T1-W MR image reveals enhancement of the entire mass, and the margin of the tumour is more clearly defined than on a postcontrast FLAIR image

Contrast enhancement on FLAIR MRI was observed in normal intracranial structures, including choroid plexus, pituitary stalk, pineal gland, dural sinuses, and cortical veins. Postcontrast T1-W imaging shows normal enhancement in the blood vessels and some intracranial structures with no blood-brain barrier, including the pineal gland, pituitary stalk, area postrema, and dura

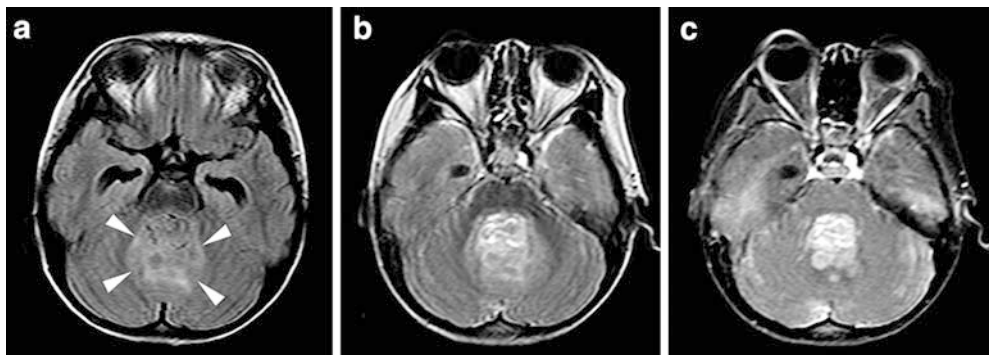


**Fig. 3a–c** A 5-year-old boy with a venous angioma. **a** A precontrast axial FLAIR MR image fails to identify the venous angioma in the left frontal lobe (*circle*). **b** Postcontrast axial FLAIR MR image reveals partial enhancement of the lesion (*circle*). **c** Postcontrast axial T1-W MR image delineates the entire extent of venous angioma owing to complete enhancement of the lesion (*circle*)

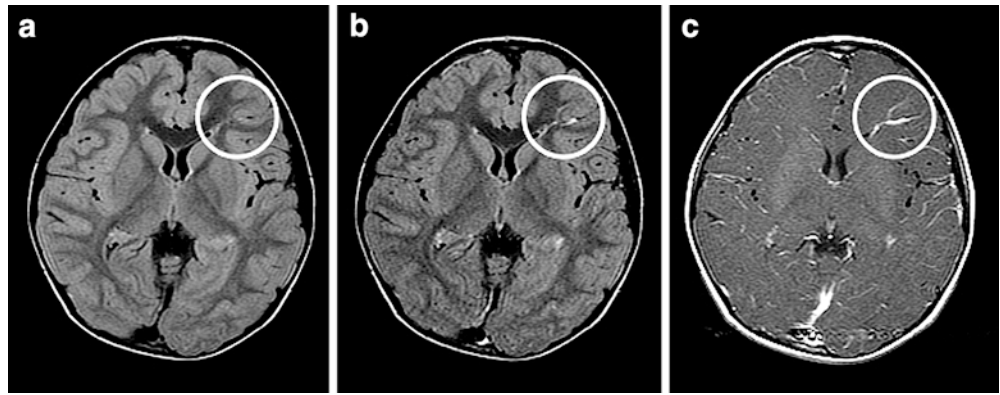
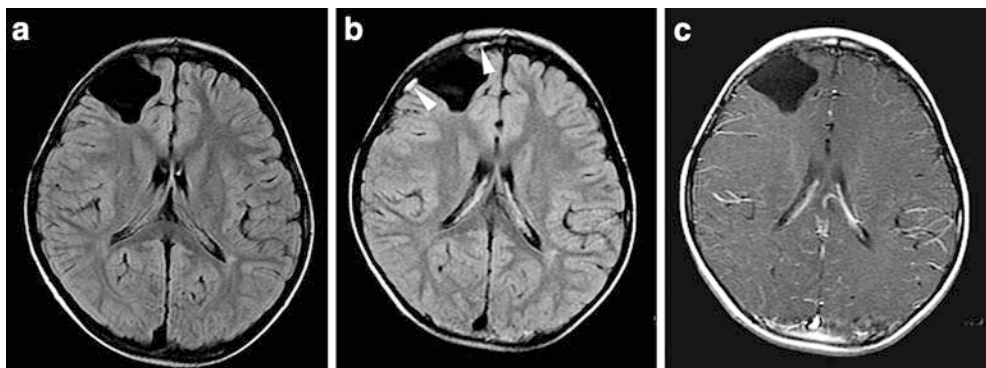


**Table 1** Lesion conspicuousness of intra-axial lesions on post-contrast FLAIR imaging

	Better	Equal	Worse	Total
Tumour	0	5	13	18
Postoperative enhancement	3	2	2	7
Inflammation	1	0	4	5
Infection	1	1	2	4
Infarction	1	1	1	3
Vascular lesions	0	0	3	3
Total	6	10	24	40

mater [23, 24]. We found that the normally enhancing intracranial structures on postcontrast FLAIR imaging were also seen on postcontrast T1-W imaging, and most blood vessels did not enhance, probably owing to a T2 effect of the FLAIR sequence. Although we did not measure the degree of enhancement, the degree of enhancement in normal intracranial structures on post-contrast FLAIR imaging appeared less intense than that on postcontrast T1-weighted imaging, probably because

**Fig. 4a–c** A 7-year-old boy with metastatic neuroblastoma. **a** Precontrast axial FLAIR MR image shows a parenchymal defect in the right frontal lobe due to excised metastatic neuroblastoma. **b** Postcontrast axial FLAIR MR image shows linear meningeal enhancement (*arrows*) around the operation site. **c** This postoperative enhancement is more conspicuous on a postcontrast FLAIR image than on a postcontrast T1-W image



of a mild T1 effect of the FLAIR sequence. Because postcontrast FLAIR images were obtained only in the axial plane, some normally enhancing structures which are not well seen in the axial plane and small in size, such as the pituitary gland and area postrema, could not be evaluated. Being aware of the normal intra-cranial enhancement on postcontrast FLAIR images may be helpful in detecting abnormal intracranial enhancement on the same sequence.

Lesion conspicuousness on postcontrast FLAIR imaging, which was compared with that of postcontrast T1-W imaging, was different according to lesion location. For all enhancing lesions, there seemed to be no definite advantage of postcontrast FLAIR imaging over postcontrast T1-W imaging. Postcontrast FLAIR imaging was frequently advantageous for extra-axial lesions, whereas it was frequently disadvantageous for intra-axial lesions. This difference in lesion conspicuousness on postcontrast FLAIR imaging between intra-axial and extra-axial lesions was statistically significant. Other investigators also found that lesion conspicuousness of extra-axial lesions was better on postcontrast FLAIR imaging than on T1-W imaging [1, 2, 8, 9, 10, 11, 12, 13]. Nevertheless, postcontrast FLAIR imaging was reported to be inferior to postcontrast T1-W imaging in depicting leptomeningeal metastasis [14] and the “ivy sign” of moyamoya disease [15]. In the present study, postcontrast FLAIR imaging seemed to be

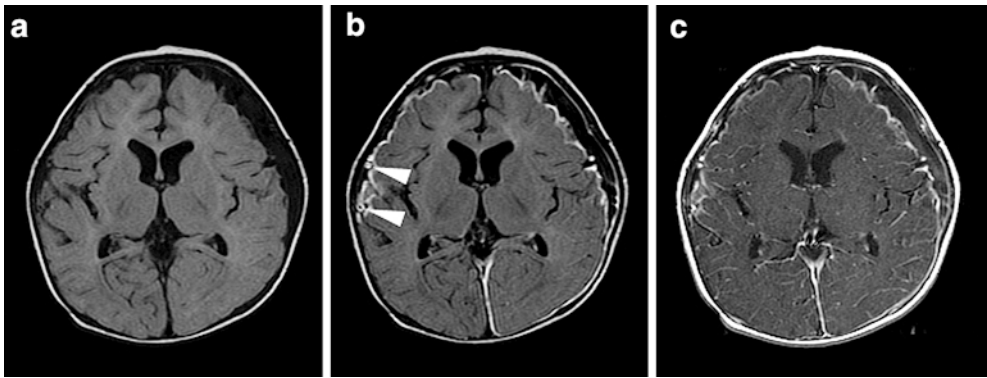


**Fig. 5a–c** A 6-month-old girl with meningitis. **a** Precontrast axial FLAIR MR image shows an extra-axial fluid collection along the left cerebral hemisphere. **b** Postcontrast axial FLAIR MR image reveals diffuse leptomeningeal enhancement due to meningitis, which is more conspicuous on a postcontrast FLAIR image than on a postcontrast T1-W image (**c**). In addition, wall enhancement of the infected vessels (*arrows*, **b**) is more clearly demonstrated on a postcontrast FLAIR image. A left extra-axial fluid collection is proven to be in the subdural space because the enhancing cortical vessels are medially displaced on both postcontrast FLAIR and T1-W images

comparable to postcontrast T1-W imaging for leptomeningeal metastasis and worse than postcontrast T1-W imaging for abnormal vascular enhancement in two children with moyamoya disease. Results of intra-axial lesions on postcontrast FLAIR imaging by other investigators have been inconsistent [1, 4, 5, 6, 7].

Lesion conspicuousness on postcontrast FLAIR imaging seemed to vary according to disease category and lesion location. Among intra-axial lesions, postcontrast FLAIR imaging was disadvantageous in depicting tumour, inflammatory lesions, and vascular lesions. Among extra-axial lesions, postcontrast FLAIR imaging was advantageous in depicting postoperative enhancement, meningitis, subdural haematoma and leptomeningeal angiomatosis. In contrast, it was disadvantageous in depicting extra-axial vascular lesions except for leptomeningeal angiomatosis. Interestingly, leptomeningeal angiomatosis revealed better lesion

conspicuousness on postcontrast FLAIR imaging in contrast to other vascular lesions, including venous angioma, arteriovenous malformation, leptomeningeal collaterals in moyamoya disease, and increased vascular enhancement in acute infarction. Based on this observation, we speculate that blood flow in leptomeningeal angiomatosis may be slower than in other vascular lesions. Therefore, postcontrast FLAIR imaging may be helpful in depicting leptomeningeal angiomatosis in patients with Sturge-Weber syndrome. Postcontrast FLAIR imaging may also be helpful in detecting chronic subdural haematoma because the lesion may be detected only on that sequence. Furthermore, abnormal wall enhancement of the infected vessel in meningitis was clearly seen on post-contrast FLAIR imaging. However, any generalisation of our results on lesion conspicuity according to disease category is limited by the small number in each category in our study and may indicate only trends or suggestions.

Differences in lesion conspicuity between postcontrast FLAIR imaging and postcontrast T1-W imaging may be explained by a combination of a different T1 shortening effect to a certain concentration of gadopentetate dimeglumine and a different T2 effect according to the different vascularity of a lesion. In the present study, three postcontrast T1-W imaging techniques were used and they may have had different effects on contrast enhancement. The fat-suppression technique

**Fig. 6a–c** A 10-month-old girl with a subdural hematoma. **a** A precontrast axial FLAIR MR image shows the subdural hematoma (*arrowheads*) in the left temporal lobe, which is hyperintense to cerebrospinal fluid. **b** A postcontrast axial FLAIR MR image reveals more extensive enhancement of the subdural hematoma (*arrowheads*) than that on **c** a post-contrast T1-weighted image

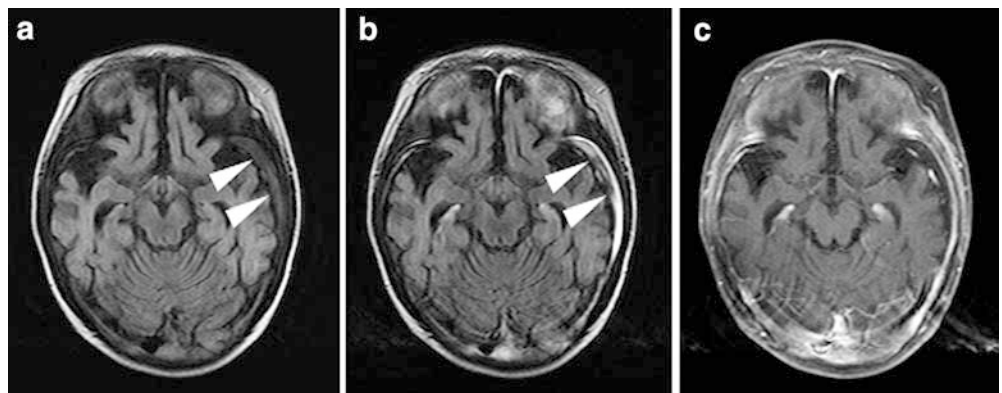


**Table 2** Lesion conspicuousness of extra-axial lesions on post-contrast FLAIR imaging

	Better	Equal	Worse	Total
Postoperative enhancement	14	6	2	22
Meningitis	9	4	1	14
Subdural haematoma	7	4	1	12
Leptomeningeal metastasis	4	2	5	11
Leptomeningeal angiomatosis <sup>a</sup>	3	1	0	4
Other vascular lesions	0	0	3	3
Epidural haematoma	0	1	0	1
	36	18	13	67

<sup>a</sup>Four patients with leptomeningeal angiomatosis were separately described because lesion conspicuity on postcontrast FLAIR MRI seemed to be better than those of other vascular lesions

mainly decreases the signal intensity of fat-containing extracranial structures, including the scalp, calvarium, and orbit, because intracranial fat is normally absent. The magnetisation transfer technique increases the

conspicuity of enhancing lesions by suppressing signal intensity of the brain parenchyma. Therefore, we think that the application of magnetisation transfer pre-pulse on T1-W sequence may not reduce the advantage of postcontrast FLAIR images in the assessment of extra-axial lesions in children.

A limitation of our study was the variable echo train lengths used for FLAIR sequence because a long echo train induces magnetization transfer saturation effects and subsequently improves the conspicuousness of contrast enhancement. This limitation resulted from the retrospective nature of our study, in which brain MR examinations were performed in two MR systems.

In conclusion, the choroid plexus, pituitary stalk, pineal gland, dural sinuses, and cortical veins show normal enhancement on postcontrast FLAIR MRI in children. Postcontrast FLAIR imaging appears to be better than postcontrast T1-W imaging in the assessment of extra-axial enhancing lesions and worse in the assessment of intra-axial enhancing lesions.

## References

- Mathews VP, Caldemeyer KS, Lowe MJ, et al (1999) Brain: gadolinium-enhanced fast fluid-attenuated inversion recovery MR imaging. *Radiology* 211:257–263
- Mamourian AC, Hoopes PJ, Lewis LD (2000) Visualization of intravenously administered contrast material in the CSF on fluid-attenuated inversion-recovery MR images: an in vitro and animal-model investigation. *AJNR* 21:105–111
- Jackson EF, Hayman LA (2000) Meningeal enhancement on fast FLAIR images. *Radiology* 215:922–924
- Essig M, Schlemmer HP, Tronnier V, et al (2001) Fluid-attenuated inversion-recovery MR imaging of gliomatosis cerebri. *Eur Radiol* 11:303–308
- Essig M, Metzner R, Bonsanto M, et al (2001) Postoperative fluid-attenuated inversion recovery MR imaging of cerebral gliomas: initial results. *Eur Radiol* 11:2004–2010
- Tsuchiya K, Mizutani Y, Hachiya J (1996) Preliminary evaluation of fluid-attenuated inversion-recovery MR in the diagnosis of intracranial tumors. *AJNR* 17:1081–1086
- Essig M, Knopp MV, Schoenberg SO, et al (1999) Cerebral gliomas and metastases: assessment with contrast-enhanced fast fluid-attenuated inversion-recovery MR imaging. *Radiology* 210:551–557
- Misaki K, Nakada M, Hayashi Y, et al (2001) Contrast-enhanced fluid-attenuated inversion recovery MRI is useful to detect the CSF dissemination of glioblastoma. *J Comput Assist Tomogr* 25:953–956
- Kanamalla US, Baker KB, Boyko OB (2001) Gadolinium diffusion into subdural space: visualization with FLAIR MR imaging. *AJR* 176:1604–1605
- Bozzao A, Floris R, Fasoli F, et al (2003) Cerebrospinal fluid changes after intravenous injection of gadolinium chelate: assessment by FLAIR MR imaging. *Eur Radiol* 13:592–597
- Tsuchiya K, Katase S, Yoshino A, et al (2001) FLAIR MR imaging for diagnosing intracranial meningeal carcinomatosis. *AJR* 176:1585–1588
- Bozzao A, Bastianello S, Bozzao L (1997) Superior sagittal sinus thrombosis with high-signal-intensity CSF mimicking subarachnoid hemorrhage on MR FLAIR images. *AJR* 169:1183–1184
- Dechambre SD, Duprez T, Grandin CB, et al (2000) High signal in cerebrospinal fluid mimicking subarachnoid hemorrhage on FLAIR following acute stroke and intravenous contrast medium. *Neuroradiology* 42:608–611
- Singh SK, Leeds NE, Ginsberg LE (2002) MR imaging of leptomeningeal metastases: comparison of three sequences. *AJNR* 23:817–821
- Yoon HK, Shin HJ, Chang YW (2002) “Ivy sign” in childhood moyamoya disease: depiction of FLAIR and contrast-enhanced T1-weighted MR images. *Radiology* 223:384–389
- Noguchi K, Ogawa T, Inugami A, et al (1995) Acute subarachnoid hemorrhage: MR imaging with fluid-attenuated inversion recovery pulse sequences. *Radiology* 196:773–777
- Noguchi K, Ogawa T, Seto H, et al (1997) Subacute and chronic subarachnoid hemorrhage: diagnosis with fluid-attenuated inversion-recovery MR imaging. *Radiology* 203:257–262
- Singer MB, Atlas SW, Drayer BP (1998) Subarachnoid space disease: diagnosis with fluid-attenuated inversion-recovery MR imaging and comparison with gadolinium-enhanced spin-echo MR imaging—blinded reader study. *Radiology* 208:417–422
- Husstedt HW, Sickert M, Köstler H, et al (2000) Diagnostic value of the fast-FLAIR sequence in MR imaging of intracranial tumors. *Eur Radiol* 10:745–752
- Tsuchiya K, Inaoka S, Mizutani Y, et al (1997) Fast fluid-attenuated inversion-recovery MR of intracranial infections. *AJNR* 18:909–913

- 
21. Sie LT, Barkhof F, Lefeber HN, et al (2000) Value of fluid-attenuated inversion recovery sequences in early MRI of the brain in neonates with a perinatal hypoxic-ischemic encephalopathy. *Eur Radiol* 10:1594–1601
  22. Frigon C, Jardine DS, Weinberger E, et al (2002) Fraction of inspired oxygen in relation to cerebrospinal fluid hyperintensity on FLAIR MR imaging of the brain in children and young adults undergoing anesthesia. *AJR* 179:791–796
  23. Berry I, Brant-Zawadzki M, Osaki L, et al (1986) Gd-DTPA in clinical MR of the brain. 2. Extraaxial lesions and normal structures. *AJR* 147:1231–1235
  24. Kilgore DP, Breger RK, Daniels DL, et al (1986) Cranial tissues: normal MR appearance after intravenous injection of Gd-DTPA. *Radiology* 160:757–761